Analytically tractable studies of traveling waves of activity in integrate-and-fire neural networks

Jie Zhang[1] and Remus Osan[1,2,*]

[1]*Department of Mathematics and Statistics, Georgia State University, Atlanta, Georgia 30303, USA*

[2]*Neuroscience Institute, Georgia State University, Atlanta, Georgia 30093, USA*

(Received 9 December 2015; published 27 May 2016)

In contrast to other large-scale network models for propagation of electrical activity in neural tissue that have no analytical solutions for their dynamics, we show that for a specific class of integrate and fire neural networks the acceleration depends quadratically on the instantaneous speed of the activity propagation. We use this property to analytically compute the network spike dynamics and to highlight the emergence of a natural time scale for the evolution of the traveling waves. These results allow us to examine other applications of this model such as the effect that a nonconductive gap of tissue has on further activity propagation. Furthermore we show that activity propagation also depends on local conditions for other more general connectivity functions, by converting the evolution equations for network dynamics into a low-dimensional system of ordinary differential equations. This approach greatly enhances our intuition into the mechanisms of the traveling waves evolution and significantly reduces the simulation time for this class of models.

DOI: 10.1103/PhysRevE.93.052228

I. INTRODUCTION

Traveling waves of electrical activity have been widely observed and measured in various brain regions under both spontaneous and evoked conditions, for example, in the visual [1–6], olfactory [7,8], auditory [9,10], somatosensory [11], and motor cortices [12]. These traveling waves are thought to play an important role in sensory processing [13], phase coding [14,15], and sleep [16]. Research also suggests the existence of traveling waves for hippocampal theta oscillations which may act as local clocks to govern spatial-temporal dynamics [17,18]. This area of research is essential not only for understanding the functions of the brain during sensory processing, but also for providing insights into irregular neural dynamics [19] or abnormal states such as epileptic seizure [20,21], migraine [22], hallucination [23,24], and the ones observed after brain injury [25].

Computational models are essential for the understanding of traveling waves in neural tissue, yet the lack of analytical solutions for the dynamics of activity propagation detracts from their usefulness. These models usually describe the neural tissue as a vast interconnected network of homogeneous excitatory units, such as firing rate models [26–29], integrate and fire models [26,30–35], theta neuron models [36,37], or more complex models of neurons [30,38–45]. In these models, propagating waves have been studied numerically in an extensive fashion using the assumptions that the strength of the synaptic connections between neurons depends only on the distance between them. Typically, these models give rise to a pair of traveling wave speed solutions, where the slower wave is unstable, and the fast one is stable. The assumptions listed above make it possible to formulate a set of integro-differential equations describing the propagation of the one-spike traveling wave fronts in a continuous one-dimensional integrate-and-fire network. Using these equations, we have derived the transition between initiation and evolution toward constant speed traveling waves for Gaussian connectivity [32] and finite support connectivity [34]. We confirmed these findings through numerical simulations, leading to methods for optimizing and improving simulations of large-scale networks [35], and we extended these results for the case of constant speed waves with a finite and an infinite number of spikes [33].

In this paper, we formulate a system of ordinary differential equations for traveling wave propagation that examines the evolution of first, second, and potentially higher order derivatives of firing times as a function of space. For a specific choice of the spatial connectivity and the time evolution of the spike-induced synaptic excitation, the consequence of expressing the set of evolution equations in this analytically tractable form is that the dynamics of the traveling waves depend on local dynamics. This is a very surprising result since the excitation due to one neuron spiking affects all other neurons in the network. Furthermore, in contrast with previous models used in this area, these evolution equations can be solved analytically. More precisely, we show that the wave acceleration depends quadratically on the instantaneous speed, which allows us to solve the equation explicitly and to exactly determine how wave velocity and acceleration change as a function of time and space. In order to obtain these analytical results we restrict our analysis to integrate and fire neurons that spike only once, that is, we examine single-spike activity propagation. We then use this model to explain the existence of three regimes of wave propagation and neural dynamics, in agreement with previous results from numerical simulations. A major finding is that propagation failure or evolution toward a stable constant speed traveling wave proceeds according to a natural time scale that depends explicitly on the network excitability parameters as well as on time scales of neural integration and excitation decay. Finally, we show that these results extend to more generalized connectivity functions that still allow for local evolution equations. Not surprisingly, when these functions are more complicated, finding analytical solutions becomes much more challenging. Nevertheless,

*rosan@gsu.edu

the use of the local evolution equations, obtained from a low-dimensional system of differential equations, drastically reduces the simulation time for the full network dynamics.

II. EVOLUTION EQUATIONS IN INTEGRATE-AND-FIRE MODEL

In this study, we seek analytical solutions for the evolution of one-spike activity propagation in a class of neural networks. Here we use a simple and widely used model for a spiking neuron, the integrate-and-fire model, which integrates the input signal with temporal constant τ_1 until its voltage reaches a threshold V_T, at which point the neuron sends an excitatory spike to the rest of the network. To describe the network interactions we make use of the following two functions. First, $J(x,y)$ describes the synaptic coupling between neurons at positions x and y. Second, $A(t)$ represents the excitation provided by a presynaptic spike onto the postsynaptic neuron. The functions $J(x,y)$ and $A(t) = A_2(t) - A_1(t)$ take the following explicit form:

$$J(x,y) = \frac{e^{\frac{-|x-y|}{\sigma}}}{2\sigma}, \qquad A(t) = \frac{e^{-\frac{t}{\tau_2}}}{1-\frac{\tau_1}{\tau_2}} - \frac{e^{-\frac{t}{\tau_1}}}{1-\frac{\tau_1}{\tau_2}}. \tag{1}$$

For function $J(x,y)$, which depends only on the absolute value of $|x-y|$, the symbol σ indicates the connectivity spatial scale. Other explicit functions for $J(x,y)$ will be considered later. For the temporal function $A(t)$, τ_2 is the time constant for the decay of the synaptic excitation, which is assumed to be greater than τ_1; also $A(t) = 0$ for $t < 0$. The membrane voltage for a neuron in the network then can be expressed in integral form [32]:

$$\frac{V(x,t)}{g_{\text{syn}}} = J \otimes A = \int_{-\infty}^{x} J(x,y)A[t - t(y)]\,dy, \tag{2}$$

where $\otimes$ denotes convolution and $t(y)$ is the spiking time for the neuron at position y. Here g_{syn} is a constant that controls the excitation of the network. It is assumed that dynamics in the network are completely determined by the excitation due to the previous neuron spikes that occur at $t(y) < t$. We note here that initiation of activity propagation may initially occur through applying an external current to a subset of neurons in the network. For example, a preferred way to do this in the numerical simulation is to induce a large group of neurons to spike at the same time, $t = 0$, and then to monitor propagation to the right of that region. For simplicity we assume that the wave propagates only in one direction, taken here to be from left to right, and we ignore neural spikes that may occur to the left of the initiation region. After integrating the excitatory signals, the firing condition of a neuron at position x, taken to be at the leading edge of the propagation, becomes $V(x,t(x)) = V_T$. Since $t(x)$ is the time at which the voltage $V(x,t)$ of neuron at position x first crosses threshold, this constitutes a consistency equation. In this one-dimensional network, it can be shown that neurons' firing time is a monotonic function of their position x; this holds true for many other classes of connectivity functions [34,35].

We take two derivatives of equation (2) with respect to x, with the goal of obtaining an equation that connects $t' = dt/dx$ and $t'' = d^2t/dx^2$:

$$\frac{d(V_T/g_{\text{syn}})}{dx} = (J \otimes A)' = J' \otimes A + (J \otimes A')t' = 0, \tag{3}$$

$$0 = J'' \otimes A + 2t'J' \otimes A' + t''J \otimes A' + (t')^2 J \otimes A'' + J_0 A_0' t', \tag{4}$$

where we used $A_0 = A(0) = 0$ in Eq. (4). The other notations used here are $J_0 = J(0) = 1/2/\sigma$ and $A_0' = A'(t=0) = 1/\tau_1$. Equations (2)–(4) constitute a system of evolution equations that shape the traveling wave propagation. In the next section, we will show how we can convert them to an ordinary differential equation.

III. ANALYTICAL SOLUTIONS

Since functions $J(x)$, $A_1(t)$, and $A_2(t)$ are all exponentials, the system of Eqs. (2)–(4) contains only two unknowns, of the form $K_1 = J \otimes A_1$ and $K_2 = J \otimes A_2$. Solving for them as a function of t' in the Eqs. (2)–(3) and substituting these solutions in (4) yields an equation where t'' is a function of t'. We obtain $J' = \frac{dJ(x)}{dx} = J/(-\sigma), A_k' = \frac{dA_k(t(x))}{dx} = A_i/(-\tau_k)t', k = 1,2$. Then we can write Eqs. (2)–(3) in a compact way:

$$\frac{V_T}{g_{\text{syn}}} = K_2 - K_1, \tag{5}$$

$$K_2\left(\frac{1}{\sigma} + \frac{1}{\tau_2}t'\right) = K_1\left(\frac{1}{\sigma} + \frac{1}{\tau_1}t'\right). \tag{6}$$

Terms K_1 and K_2 can now be determined from Eqs. (5)–(6) as functions of the instantaneous speed $c = 1/t'$:

$$K_1 = \frac{V_T}{g_{\text{syn}}}\left(\frac{c}{\sigma} + \frac{1}{\tau_2}\right)\Big/\left(\frac{1}{\tau_1} - \frac{1}{\tau_2}\right), \tag{7}$$

$$K_2 = \frac{V_T}{g_{\text{syn}}}\left(\frac{c}{\sigma} + \frac{1}{\tau_1}\right)\Big/\left(\frac{1}{\tau_1} - \frac{1}{\tau_2}\right). \tag{8}$$

After simplifications, we can rewrite Eq. (4) as a single equation that relates t'' to c:

$$\frac{d^2t_x}{dx^2} = \frac{K_1\left(\frac{1}{\sigma} + \frac{1}{c\tau_1}\right)^2 - K_2\left(\frac{1}{\sigma} + \frac{1}{c\tau_2}\right)^2 - \frac{1}{2\sigma c\tau_1}}{\frac{K_1}{\tau_1} - \frac{K_2}{\tau_2}}. \tag{9}$$

After substituting the explicit solutions for the terms K_1 and K_2 in Eq. (9), we can determine d^2t_x/dx^2 as a function of speed. As an additional step, we convert d^2t_x/dx^2 into the instantaneous acceleration, which is a more intuitive measure for the activity propagation, using the following relationship between these two quantities:

$$a(x) = \frac{d^2x}{dt_x^2} = -\frac{1}{\left(\frac{dt_x}{dx}\right)^2}\frac{d^2t_x}{dx^2}\frac{dx}{dt_x} = -c^3\frac{d^2t_x}{dx^2}. \tag{10}$$

Combining these equations, we obtain a remarkably simple analytical relationship between $a(x)$ and $c(x)$:

$$a(x) = -\frac{[c(x) - c_1][c(x) - c_2]}{\sigma}, \tag{11}$$

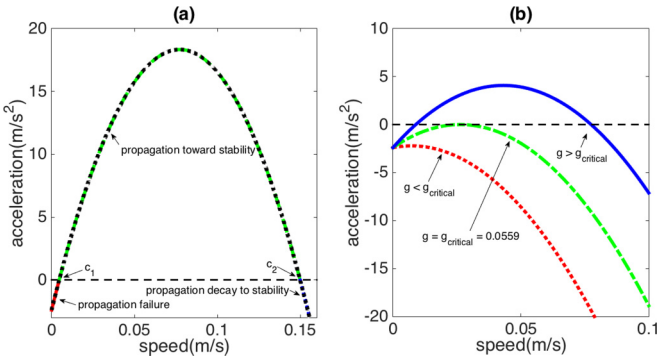

FIG. 1. (a) Theoretical results and numerical simulations for the dependence of wave acceleration on instantaneous speed, $a = a(c)$. The acceleration's quadratic dependence on speed (curve with merged blue, green, and red regions) is in perfect agreement with numerical simulations (dotted black line) on all areas except for the low speed regime where the agreement again becomes excellent with finer discretization of the spatial domain. The parameters used here are $\tau_1 = 4\,\text{ms}$, $\tau_2 = 30\,\text{ms}$, $\sigma = 0.288\,\text{mm}$, $V_T = 15\,\text{mV}$, $g_{\text{syn}} = 98.4\,\text{mV}$, yielding $c_1 = 0.0046\,\text{m/s}$, and $c_2 = 0.15\,\text{m/s}$. These parameters are in agreement with published data, and they are used as default values unless noted otherwise. (b) Theoretical results for acceleration vs speed for different excitability levels g_{syn}. Depending on the overall excitability level, there are no traveling wave solutions (red line), one solution (green line), or two solutions (blue line). As excitability increases, c_1 and c_2 decrease or increase, respectively, provided that the overall excitability exceeds the critical value $g_{\text{critical}} = 0.0559V$ [see Eq. (13)].

where c_1 and c_2 are the speed for the slow-unstable and the fast-stable constant speed traveling wave solutions, respectively. This quadratic equation is easy to visualize [Fig. 1(a)]. These constant speed wave solutions depend only on parameters σ, τ_1, τ_2, and $B = g_{\text{syn}}/(2V_t\tau_1), \beta = (\tau_1 + \tau_2)/(\tau_1\tau_2)$, shown here explicitly:

$$c_{1,2} = \sigma/2\left[B - \beta \mp \sqrt{(B-\beta)^2 - \frac{4}{\tau_1\tau_2}}\right]. \qquad (12)$$

The pair of speeds, c_1 and c_2, are real and positive for different values of network excitability g_{syn}, provided that this parameter exceeds a critical value g_{critical} [Fig. 1(b)]:

$$g_{\text{critical}} = 2V_t\tau_1\left(\frac{\tau_1+\tau_2}{\tau_1\tau_2} + \sqrt{\frac{4}{\tau_1\tau_2}}\right). \qquad (13)$$

In agreement with previous results, the decrease of the excitability parameter g_{syn} brings the two solutions c_1 and c_2 closer and closer together, until these solutions collide and cease to exist. Below g_{critical}, c_1 and c_2 become complex, and in turn, the acceleration can take only negative values, resulting in eventual propagation failure regardless of how activity propagation is initiated. This relationship is evident in Fig. 2(a), where the connection between $c_{1,2}$ and g_{syn} is illustrated. The slow-unstable wave has a horizontal speed asymptote at zero as g_{syn} goes to ∞, while the fast-stable wave has an oblique asymptote with slope σB. The same properties exhibited by Eq. (12) were found numerically [30], in agreement with later results [31,33]. The dependence of the

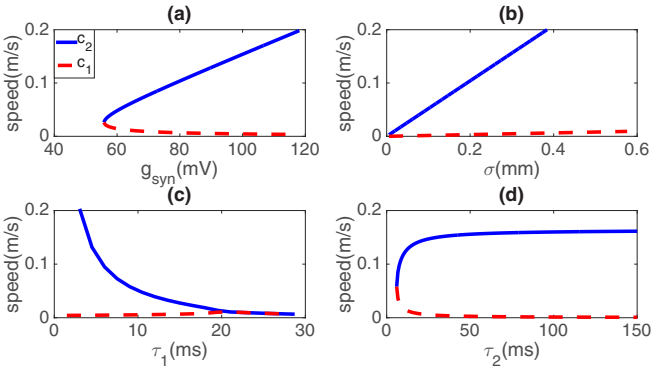

FIG. 2. Dependence of traveling wave solutions c_1 (red) and c_2 (blue) on neuron and network parameters. (a) Speed vs synaptic excitability g_{syn}, with bifurcation occurring at $g_{\text{critical}} = 0.0559\,\text{mV}$. (b) Speed vs σ, revealing linear correlations between propagating velocity and parameter σ. (c) Speed vs τ_1, showing a decrease of c_2 as the neuron integration time, τ_1, increases. (d) Speed vs τ_2, indicating that fast solutions increase with the growth of decay time, τ_2, in contrast to the slow solutions showing the opposite trend.

c_1 and c_2 on other network parameters such as connectivity footprint σ, the neuron integration time τ_1, and the decay time of synaptic excitation τ_2 is illustrated in Figs. 2(b)–2(d).

A consequence of the relationship between acceleration and speed [Eq. (11)] is that the traveling wave fails if $c < c_1$ or evolves toward $c(\infty) = c_2$ if $c > c_1$. These outcomes are illustrated in Fig. 3(a), which shows the neuronal positions versus their firing times. As a reminder, activity propagation is initiated here by inducing a large enough region to spike at $t = 0$ through the application of a sufficiently high external current to all neurons in that region. The size of the initial

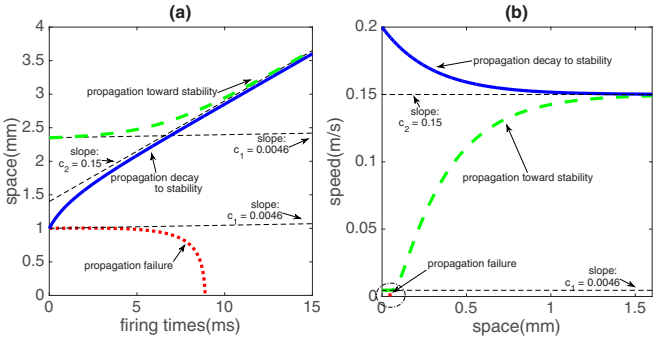

FIG. 3. (a) Space vs firing times. Different initial conditions will determine if the transients evolve toward stable or transient propagation. When the speed (tangent) is less than c_1, propagation fails as expected (red line, failure when tangent becomes vertical). When the tangent is greater than c_2 (blue line), the traveling wave slows down and evolves asymptotically toward the constant speed traveling wave indicated by slope c_2. When the tangent is greater than c_1 but less than c_2 (green line), the traveling wave speeds up and evolves asymptotically toward a fast-stable solution at c_2. Results from numerical simulations, not shown here, are in perfect agreement with color lines shown in this graph. (b) Speed vs space. In agreement with results from part (a), propagation failure is achieved in a finite amount of space, while stability at c_2 is reached asymptotically.

area, which needs to exceed a threshold value, allows us to control the initial phase of the traveling wave, as larger areas will provide more excitation to the neurons close to the initiation region, and it will consequently result in a greater initial speed for the activity propagation. In order to have stable constant wave propagation, solutions are assumed to be real, thus $(B - \frac{\tau_1+\tau_2}{\tau_1\tau_2})^2 - \frac{4}{\tau_1\tau_2} > 0$. Not surprisingly, when we examine the evolution of speed as a function of space [Fig. 3(b)], we notice again the existence of three distinct regimes: propagation failure for $c < c_1$, acceleration toward c_2 if $c > c_1$, and deceleration toward c_2 if $c > c_2$.

A. Coupling between speed and acceleration leads to wave stability

Most surprisingly, Eq. (11) reveals that the relationship between the acceleration and the instantaneous speed is independent of how the wave was initiated. More precisely, any two instances of activity propagation that achieve the same speed will follow the same future dynamics despite the fact that the prior firing maps are different. This is not a trivial result, since in principle each spike in the network exerts an influence on the rest of the network, therefore the naive intuition would be that different initial conditions would result in dissimilar activity propagation dynamics, even for the cases of speed matching at a common point in the network.

We can see from Fig. 1(a) that the two roots of the quadratic equation correspond to the constant low-speed unstable and high-speed stable traveling wave solutions. This provides a global stability explanation for why any transient propagation will evolve toward a constant speed solution with speed c_2, provided that the initial speed of the propagation is larger than c_1, or fail otherwise. When $c < c_1$ acceleration stays negative and increases in amplitude as the wave slows down toward propagation failure at $c = 0$. When $c_1 < c < c_2$ acceleration stays positive but decreases in magnitude as the wave speeds up toward the constant speed solution with $c = c_2$. When $c > c_2$ acceleration stays negative but decreases in amplitude as the wave slows down toward the constant speed solution with $c = c_2$. All these trends are true regardless of the exact value of initial speed c, therefore these results go beyond standard proofs of stability for traveling waves, which are usually done using perturbation theory [30,46], meaning that the results hold only for small perturbation around the stable constant speed traveling wave. In contrast, our stability argument holds for random shuffling of firing times or perturbations of arbitrary large amplitude in voltage, and as such are more general in nature than the ones resulting from the perturbation theory.

B. Analytical solutions and natural time scales for activity propagation

We now take advantage of this remarkable result from Eq. (11) to determine analytical expressions for $t(x)$,$c(t)$,$x(t)$, and $x(c)$. Integrating Eq. (11) after separating variables c and t, we obtain

$$t(c) = \frac{\sigma}{c_2 - c_1} \ln\left(\frac{c - c_1}{c - c_2} k\right), \tag{14}$$

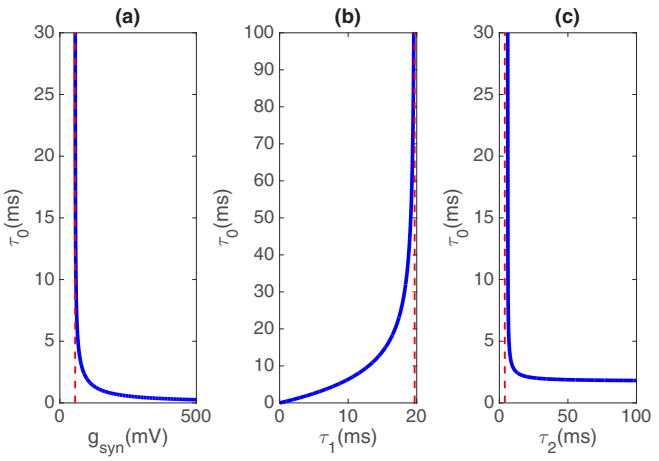

FIG. 4. Dependence of natural time scale τ_0 on other network parameters. (a) τ_0 vs g_{syn}. As the excitability of the network (g_{syn}) increases, it takes less time to achieve stability (at $c = 0$ or at $c = c_2$). Here $\tau_0 = 0.12/g_{syn}$, where $g_{syn} > g_{critical} = 55.9$ mV. (b) τ_0 vs τ_1. As the integration time τ_1 increases it takes more time to reach the stable states. When τ_1 becomes really small we obtain $\tau_0 = 0.4386\tau_1$. (c) τ_0 vs τ_2. Finally, when synaptic excitation lasts longer (at higher values of τ_2), stable states are also reached faster. When τ_2 becomes really large we obtain $\tau_0 = 1.7544$.

where $k = (c_0 - c_2)/(c_0 - c_1)$ and c_0 is the initial propagation speed at $t = 0$. Inverting $c(t)$ in Eq. (14) and using the definition $\tau_0 = \sigma/(c_2 - c_1)$ we obtain

$$c(t) = \frac{c_2 e^{t/\tau_0} - c_1 k}{e^{t/\tau_0} - k}. \tag{15}$$

Integrating both equations of (15) after separating variables x and t yields

$$x(t) = \sigma \ln\left(\frac{e^{t/\tau_0} - k}{e^{t_0/\tau_0} - k}\right) + c_1(t - t_0), \tag{16}$$

where t_0, which in general is different from 0, is the firing time of neuron located at position $x = 0$. In order to determine the speed of propagation as a function of the spatial position, we integrate Eq. (11), after separating variables x and c, also using $a(x) = dc/dt = dc/dx\, dx/dt = c\, dc/dx$:

$$x(c) = \tau_0\left[c_1 \ln\left(\frac{c - c_1}{c_0 - c_1}\right) - c_2 \ln\left(\frac{c - c_2}{c_0 - c_2}\right)\right]. \tag{17}$$

Again, theoretical results are in excellent agreement with numerical simulations for speed versus space plots [Fig. 3(b)], where all transients can be thought to be located at an initial point along the speed versus space curve. From Eqs. (15)–(16) it is clear that stability depends on the natural time scale τ_0:

$$\tau_0 = \frac{\tau_1}{\sqrt{\left(1 + \frac{\tau_1}{\tau_2} - \frac{g_{syn}}{2V_t}\right)^2 - 4\frac{\tau_1}{\tau_2}}}. \tag{18}$$

Based on this formula, it is easy to infer how τ_0 depends on these network constants. If $g_{syn} \to \infty$, $\tau_0 = \mathcal{O}(g_{syn}^{-1})$, with constant slope $2V_t\tau_1$ [Fig. 4(a)]. As τ_1 decreases toward zero, we obtain $\lim_{\tau_1 \to 0} \tau_0 = 0$ [Fig. 4(b)]. Furthermore, as the synaptic decay constant τ_2 increases toward large values, we obtain $\lim_{\tau_2 \to \infty} \tau_0 = 2V_t/g_{syn}\tau_1$ [Fig. 4(c)].

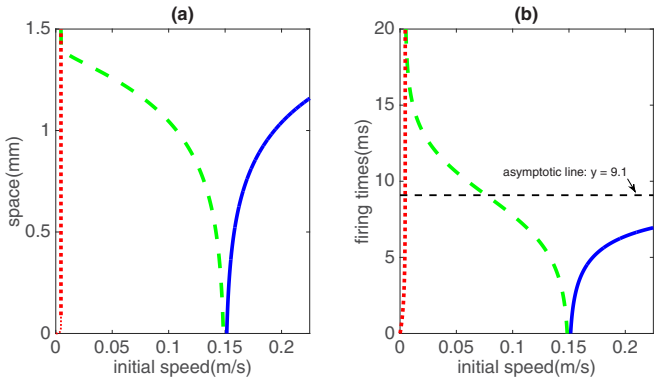

FIG. 5. (a) Spatial scales for achieving stable states. We examine the distance needed to achieve stability depends on the initial speed c_0. For propagation failure, this is defined as the distance traveled until speed becomes 0 (red line). For the asymptotically stable states, this is defined as the distance needed to reach $c = \alpha c_2$, where $\alpha = 0.99$ if $c_0 < c_2$ (green line), and $\alpha = 1.01$ if $c_0 > c_2$ (blue line). (b) Temporal scales for achieving stable state. Similar graphs are shown for the time needed to achieve stable states. In the limit where $c_0 \to \infty$ (black dotted line) stability is achieved in a finite amount of time ($t = 9.1$ ms).

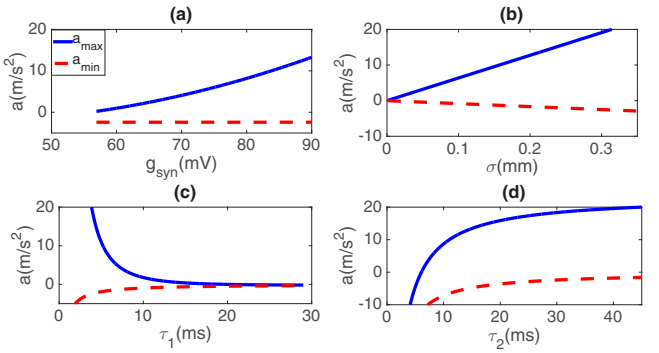

FIG. 6. Dependence of traveling-wave acceleration on parameters. (a) Acceleration vs $g_{\rm syn}$. The maximum value for acceleration (blue line) increases with excitability while surprisingly the minimum value (red line, achieved at $c = 0$ when propagation fails) does not depend on $g_{\rm syn}$. (b) Acceleration vs synaptic footprint σ. Both maximum and minimum acceleration are linear in σ. (c) Acceleration vs integration time τ_1. As the neural integration time becomes very large, both maximum and minimum acceleration decay toward zero values. (d) Acceleration vs decay of excitability parameter τ_2. In contrast, only the minimum acceleration decays to zero as τ_2 becomes large, as maximum acceleration saturates to a nonzero fixed value.

C. Reaching steady states

We now use the explicit dependence between x,t and c to determine how quickly dynamics reach the stable regimes of activity propagation, namely, propagation failure at $c = 0$ or constant speed propagation at $c = c_2$. More precisely, we want to determine where does the propagation stops and the amount of time it takes to achieve propagation failure. Similarly, when the initial speed is above c_1, we seek to determine the distance and time that will be needed for the propagation to reach stability, defined as reaching a value which is close to c_2, namely, $\alpha\, c_2$, $\alpha \approx 1$. If the initial value for propagation speed is less than c_2 we take $\alpha < 1$, otherwise we choose $\alpha > 1$. The dependence of these distances as a function of the initial speed c_0 is shown in Fig. 5(a), while the times to reach stability are shown in Fig. 5(b).

Using Eq. (17), we obtain the following analytical result about the amount of space needed to reach asymptotic stable state:

$$x(c = \alpha c_2) = \tau_0 \ln\left[\frac{(\alpha c_2 - c_1)^{c_1}}{(\alpha c_2 - c_2)^{c_2}}\right]\left[\frac{(c_0 - c_2)^{c_2}}{(c_0 - c_1)^{c_1}}\right]. \quad (19)$$

This reveals that when initial speed is very large, the amount of traveling space required to evolve towards stability also becomes very large, since $\lim_{c_0\to\infty} x(c = \alpha c_2) = \infty$. Along similar lines, using Eq. (14), we can compute the amount of time needed to reach stability as follows:

$$t(c = \alpha c_2) = \tau_0 \ln\left(\frac{\alpha c_2 - c_1}{\alpha c_2 - c_2}\frac{c_0 - c_2}{c_0 - c_1}\right). \quad (20)$$

In contrast with the amount of space needed to reach the stable state, when c_0 is very large, only a finite time is needed in order to reach stability, since $\lim_{c_0\to\infty} t(c = \alpha c_2) = \tau_0 \ln[(\alpha c_2 - c_1)/(\alpha c_2 - c_2)]$, where $\alpha > 1$.

In addition, we determine that upon reaching $c = 0$, the acceleration of the wave reaches a minimum value that does not depend on the excitability of the tissue g, that is, $a_{\rm min}(g) = -\sigma/(\tau_1\tau_2)$. We note here that this is not a global minimum, since at the other end of the spectrum, as speed becomes very large the acceleration goes to minus infinity. Finally, we note that the maximum positive acceleration, obtained at speed $(c_1 + c_2)/2$, is determined by the following equation:

$$a_{\rm max}(g_{\rm syn}) = \sigma\left[\left(B - \frac{\tau_1 + \tau_2}{\tau_1\tau_2}\right)^2 - \frac{4}{\tau_1\tau_2}\right]\Big/4. \quad (21)$$

The dependence of $a_{\rm max}$ and $a_{\rm min}$ as a function of parameters $g_{\rm syn}$, σ, τ_1, and τ_2 is shown in Fig. 6.

D. Application: Propagation changes in the presence of a connectivity gap

We consider now a small section of nonexcitable gap region that can be thought to be the result of local dead tissue. We are interested to determine the conditions that lead to activity propagation failure for a wave with an instantaneous speed $c > c_1$ that at $t = t_0$ reaches a nonexcitable gap of length L located at position x_0. Due to the choice of the exponential kernel for the synaptic connectivity, the voltage of the first neuron past the nonexcitable gap, located at $x_1 = x_0 + L$ is

$$V(x_0 + L,t) = g_{\rm syn}\int_{-\infty}^{x_0} e^{-\frac{L}{\sigma}} e^{-\frac{x_0 - y}{\sigma}} A[t - t(y)]\, dy. \quad (22)$$

At $t = t_0$ we obtain from Eq. (22)

$$V(x_0 + L,t_0) = g_{\rm syn}(K_2 - K_1)e^{-\frac{L}{\sigma}} = V_T e^{-\frac{L}{\sigma}}, \quad (23)$$

where the variables K_1 and K_2 depend on the pre-gap speed c as defined in Eqs. (5)–(6). The time dependence of the voltage of neuron at position x_1 becomes

$$V(x_1,t) = g_{\rm syn}\left(K_2 e^{-\frac{t - t_0}{\tau_2}} - K_1 e^{-\frac{t - t_0}{\tau_1}}\right)e^{-\frac{L}{\sigma}}. \quad (24)$$

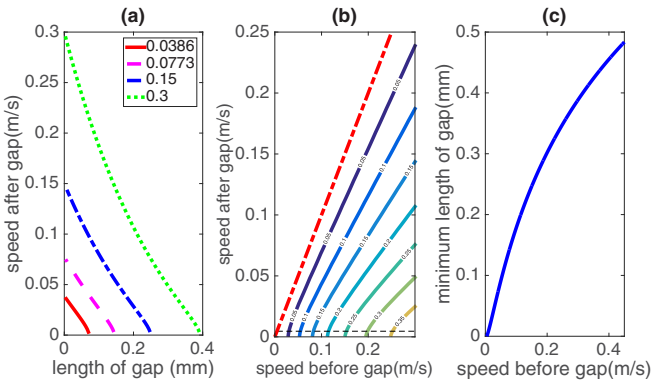

FIG. 7. Activity propagation changes induced by a nonexcitable region of length L. (a) Speed after gap vs length of gap. Not surprisingly, larger nonexcitable regions decrease the speed of the traveling waves past the gap, and they could even lead to propagation failure at $c = 0$. We plot this relationship for four initial conditions: $c = 0.0386$, $c = 0.0773$, $c = 0.15$, and $c = 0.3$. (b) Speed after gap vs speed before gap. Slow traveling waves are more affected by a constant length gap and may even fail, while fast ones only show a moderate loss in speed as they propagate further away. The red dotted line is the $y = x$, corresponding to zero speed loss, and it is included here for comparison with the other contour lines. Obviously, with the increase of gap length, the change rate of speed before and after gap increases. Length of the gaps considered here range from $L = 0.05$ to 0.35 mm, with eight uniformly spaced values considered here. (c) Minimum length of gap that causes propagation failure as a function of the speed before gap. We determine that propagation eventually fails when speed becomes less than c_1. Taking into account the speed before gap, the graph determines the minimum length of gap needed to reach propagation failure.

The neuron at position x_1 needs an additional time interval $\Delta t = \Delta t(L)$ in order to integrate the excitable current received so far and reach the threshold V_T:

$$V(x_0 + L, t_0 + \Delta t) = g_{\text{syn}}\left(K_2 e^{-\frac{\Delta t}{\tau_2}} - K_1 e^{-\frac{\Delta t}{\tau_1}}\right)e^{-\frac{L}{\sigma}} = V_T. \quad (25)$$

In general, Eq. (25) does not have an analytical solution, but numerical solutions however can be easily obtained. Following the procedure outlined in Eqs. (5)–(6), we obtain a first order equation in the speed of propagation after passing the gap, c_{gap}:

$$K_2\left(\frac{1}{\sigma} + \frac{1}{c_{\text{gap}}\tau_2}\right)e^{-\frac{\Delta t}{\tau_2}} = K_1\left(\frac{1}{\sigma} + \frac{1}{c_{\text{gap}}\tau_1}\right)e^{-\frac{\Delta t}{\tau_1}}. \quad (26)$$

The solution for $c_{\text{gap}} = c_{\text{gap}}(c, L)$ then becomes

$$c_{\text{gap}}(c, L) = \sigma \frac{\frac{K_1(c)}{\tau_1}e^{-\frac{\Delta t(L)}{\tau_1}} - \frac{K_2(c)}{\tau_2}e^{-\frac{\Delta t(L)}{\tau_2}}}{K_2(c)e^{-\frac{\Delta t(L)}{\tau_2}} - K_1(c)e^{-\frac{\Delta t(L)}{\tau_1}}}. \quad (27)$$

The failure condition after passing the gap is simply $c_{\text{gap}}(c, L) < c_1$. Numerical results for these conditions are illustrated, for fixed c in Fig. 7(a) and for fixed L in Fig. 7(b). In addition, we compute the minimum amount of nonexcitable gap that would prevent any further propagation of activity for waves that reach the gap with speed c, as shown in Fig. 7(c).

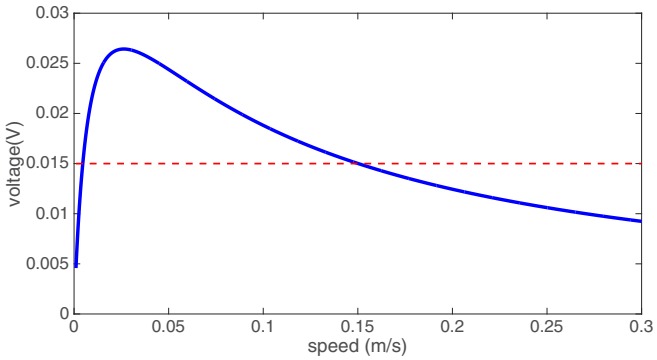

FIG. 8. Voltage value at the edge of a forced constant speed traveling wave in a network with a polynomial time exponential coupling function. A more general coupling function (28) is applied to the system with parameters $a = 1, b = 1, \tau_1 = 4 \times 10^{-3}$ s, $\tau_2 = 3.0 \times 10^{-2}$ s, $\sigma = 2.88 \times 10^{-4}$ m, $g_{\text{syn}} = 9.85 \times 10^{-2}$ V, $V_T = 1.5 \times 10^{-2}$ V. Two speed solutions exist when voltage reaches threshold ($V_T = 1.5 \times 10^{-2}$ V).

IV. APPLICATIONS TO MORE GENERAL CONNECTIVITY FUNCTION

The analytical results obtained so far depend on the specific choice of an exponential form for the connectivity function. However, our approach can be extended to more general classes of functions. We now consider a more complicated spatial connectivity function, a first order polynomial times the exponential function:

$$J(x, y) = J_1 + J_2 = \frac{a|x - y|e^{\frac{-|x-y|}{\sigma}}}{2\sigma(a\sigma + b)} + \frac{b\, e^{\frac{-|x-y|}{\sigma}}}{2\sigma(a\sigma + b)}. \quad (28)$$

A consistency equation for a wave that comes from $-\infty$ with speed c can be obtained by using $t^*(x) = x/c$. Without loss of generality, at $t = 0$ the wave will pass through $x = 0$. Therefore, we obtain $V(0,0) = V_T$, and we express it as

$$V_T = g_{\text{syn}} \int_{-\infty}^{0} \frac{a|y| + b}{2\sigma(a\sigma + b)} e^{\frac{-|y|}{\sigma}} \frac{e^{\frac{-|y|}{c\tau_2}} - e^{\frac{-|y|}{c\tau_1}}}{1 - \frac{\tau_1}{\tau_2}}\, dy. \quad (29)$$

We can then express the membrane voltage as a function of speed:

$$V(c) = \frac{g_{\text{syn}}}{2\sigma(a\sigma + b)\left(1 - \frac{\tau_1}{\tau_2}\right)}\left[\frac{a\sigma}{\left(\frac{1}{\sigma} + \frac{1}{c\tau_2}\right)^2} - \frac{a\sigma}{\left(\frac{1}{\sigma} + \frac{1}{c\tau_1}\right)^2} + \frac{b}{\frac{1}{\sigma} + \frac{1}{c\tau_2}} - \frac{b}{\frac{1}{\sigma} + \frac{1}{c\tau_1}}\right]. \quad (30)$$

Equation $V(c) = V_T$ can be written as a fourth order polynomial equation. We choose similar parameters to the exponential case in order to obtain a stable traveling wave with exact the same fast-stable speed (Fig. 8). It is easy to see when speed goes to either 0 or ∞ the membrane potential V(c) becomes 0. This guarantees that for large enough global network excitability g_{syn} there will be at least two traveling waves solutions.

We now follow the same procedure for the exponential case, namely generate enough derivatives of the original equation

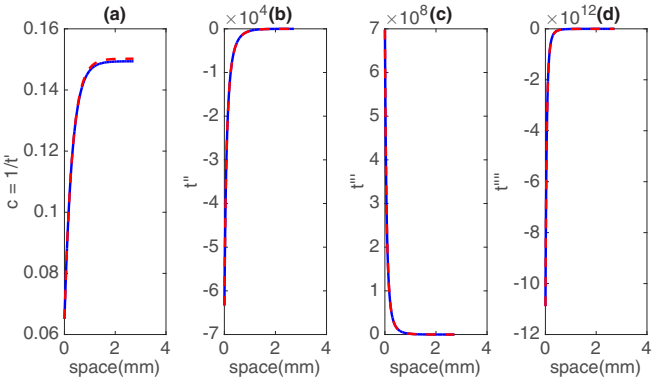

FIG. 9. Successive derivatives of firing times. Numerical simulations (blue) are in excellent agreement with the the dynamics of ODE system, as illustrated by the first four derivatives of firing map [Eqs. (2)–(4), (31)–(32), red lines]: (a) t', (b) t'', (c) t''', and (d) t''''. Similar to the previous cases considered, an initial region is induced to spike to the left of $x > 0$ region in order to provide the initial activity propagation. This is used to extract the initial conditions for the ODE system, such as the initial speed, $1/t'(0)$ as well as the next two derivatives, $t''(0)$ and $t'''(0)$.

in order to solve all convolution terms as function of the time derivatives t',t'' and higher order terms. We use these terms in order to obtain an equation that contains only these derivatives, that is, $t^{(n)} = f(t',t'',\ldots,t^{(n-1)})$. Because the system of three Eqs. (2)–(4) contains four unknowns, $J_i \otimes A_j$ ($\{i,j\} \in \{1,2\}$), only two computation of an extra derivative is needed, since due to the specific form of the connectivity kernel no new kind of functions will be created as a result of taking the derivatives of the spatial function J. These unknowns can be computed as function of t',t'', and t''' using three Eqs. (2)–(4) along with an extra derivative of Eq. (4):

$$\begin{aligned}(J\otimes A)''' = {} & J'''\otimes A + 3t'J''\otimes A' + 3(t')^2J'\otimes A'' \\ & + t'''J\otimes A' + (t')^3J\otimes A''' + 3t''J'\otimes A' \\ & + t't''J\otimes A'' + 2t'J_0'A_0' \\ & + 2t''J_0A_0' + (t')^2J_0A_0'' = 0. \end{aligned} \tag{31}$$

One additional equation, namely the derivative of Eq. (31), will connect the fourth-order derivative of the firing map $t(x)$ with the lower order derivatives of t. This yields an ordinary differential equation similar to the case analyzed earlier:

$$\begin{aligned} & J''''\otimes A + 4(t')^3J'\otimes A''' + 4t'''J'\otimes A' + 4t'J'''\otimes A' \\ & + 6t''J''\otimes A' + 6(t')^2J''\otimes A'' + 3(t'')^2J\otimes A'' \\ & + (t')^4J\otimes A'''' + t''''\cdot J\otimes A' + 4t't'''J\otimes A'' \\ & + 6(t')^2t''J\otimes A''' + 12t't''J'\otimes A'' \\ & + 5t''J_0'A_0' + 2t'''J_0A_0' + 3t't''J_0A_0'' + 3t'J_0''A_0' \\ & + 3(t')^2J_0'A_0'' + (t')^3J_0A_0''' + t't''J_0A_0' = 0. \end{aligned} \tag{32}$$

We verified that network dynamics are in agreement with this ODE system, using numerical simulations to compute values for the first three derivatives of t as initial conditions and making use of the explicit solution $t'''' = f(t',t'',t''')$ from Eq. (32), as illustrated in Fig. 9. Although the transition toward constant speed waves is now much more complicated and analytical solutions do not likely exist for this case, again local dynamics determine the evolution of the wave. More precisely, two waves that have the same values for the first three derivatives of t at a spatial location x_0 will follow identical trajectories for $x > x_0$.

This approach works for any synaptic connectivity function J who is a product of a polynomial in x and the exponential function, since no new functions will be generated through higher order derivatives of function J. Here the number of equations needed to transform the evolution equation into an ODE is $2n+3$, where n is the degree of the polynomial, with $2n+2$ derivatives of original Eq. (2) needed. In fact, this approach works for any function J that generates a finite set of functions through the process of taking derivatives. For example, combinations of polynomials, sine and cosine functions times the exponential, would also generate a finite set of functions through derivative steps. One function that cannot be used is the Gaussian function $J(x) = e^{(-x^2/(2\sigma^2))}/\sqrt{2\pi\sigma}$, since at each step of the procedure the computation of higher order derivatives keeps generating new functions such as $xe^{-x^2/(2\sigma^2)}$, $x^2e^{-x^2/(2\sigma^2)}$ and higher order polynomials times the original Gaussian function. As a result, it is not possible to solve and express the convolution unknowns as functions of derivatives of t. Nevertheless, the more advantageous property of continuous first order derivative that the Gaussian function has over the exponential kernel, can be offset by properly chosen set of functions such as $(1+|x|)e^{-|x|}$. Therefore, somehow surprisingly, activity propagation depends on local quantities only for longer range kernels such as products of polynomial and exponential functions, but not for Gaussian and other similar, more localized, types of functions. In effect, the more localized kernels ensure that the local details of the firing map are essential for further propagation, while the longer range kernels analyzed here ensure that a neighborhood of neurons close to firing is less susceptible of the details of the excitation that brought them close to the threshold.

V. CONCLUSIONS AND FUTURE DIRECTIONS

In conclusion, we have established that for the neural network models with exponential synaptic connectivity functions, the instantaneous acceleration depends only on a quadratic function of the instantaneous speed of the propagation. This is a compelling and surprising result since in principle each neural spike influences the rest of the network and would seemingly be needed to be accounted when solving for the exact network dynamics. To our knowledge, this is the first such result of its kind, since other related models do not have analytical solutions for activity propagation.

The quadratic dependence on speed provides a clear explanation of why this type of neural network can sustain two types of traveling waves, a slow-unstable wave as well as a fast-stable wave, while ruling out other possible solutions. Furthermore, this approach provides a global explanation of the traveling wave stability. When the propagation dips below the slow-unstable speed c_1, a negative acceleration will further reduce the speed until the propagation fails. In contrast, the propagation speeds up or down toward the fast-stable traveling wave c_2, depending on if the initial velocity is below or above c_2, respectively. It is not possible to achieve this level of insight

into the stability of traveling waves from other models since proofs of their stability rely on perturbation theory.

Another fundamental result of our model is that evolution toward propagation failure or constant speed traveling wave is determined by a natural global time scale. This parameter depends only on the neuron integration time τ_1, the time constant for the decay of the excitation τ_2, and on the ratio between the global excitation constant g_{syn} and the voltage threshold V_t. This provides an easy way of quantifying how fast dynamics of neural spikes evolve toward the stable states of either propagation failure or constant speed traveling wave.

Finally, these analytical results can then be directly used to derive conditions for propagation failure in presence of a gap. Not surprisingly, a small to moderate gap reduces the speed of the propagation by an amount that is small enough to allow recovery toward the fast-stable traveling wave. In contrast a large gap would either block propagation altogether or would result in a wave that jumps the gap but has a speed that is below the slow-unstable solution and it will eventually fail.

These results can be extended for more general kernels, provided that the derivatives of the spatial and temporal kernels generate a finite set of functions. Under these assumptions, the evolution equations for the propagation of activity in the neural network can be converted to a system of ordinary differential equations, with dynamics depending on the local conditions derived from a finite number of derivatives of the firing map $t(x)$. It is fascinating that despite the long-range connections considered in these models, evolution of these waves follows local rules for their dynamics. It is also quite unexpected that this is the case for longer range kernel such as exponential functions, but not for the more compact kernels such as Gaussian functions, since naively it would seem that the longer the range the more likely a neuron spike would influence the dynamics of the whole network.

In addition to improving our insight into the mechanism of these traveling waves, this approach has the potential to significantly improve the simulation time for large-scale networks. Instead of maintaining the state of all neurons in the working memory during simulations, one needs to simulate only a system of ordinary differential equations for the position of the traveling wavefront, resulting in substantial reduction of the simulation time.

Our approach can be extended for multiple-spike activity propagation. More precisely, one can obtain an infinite system of equations that contains first and second derivatives for all traveling wavefronts. Some of the effects induced by the multispike features are intuitive: the first wavefront now receives additional excitation due to the upcoming waves, excitation which depends on the separation between waves and is influenced by the relative speed by which they travel locally. Other effects are more complicated. For example, the reset condition will induce a coupling between an exponentially decaying function of the last interspike interval for each wave, except the wavefront, and the first and second order derivatives of firing times of all other evolving waves, This drastically complicates the structure of the system of evolution equations. Furthermore, this system of equations for the infinite number of wavefronts has to be solved simultaneously, which renders the search for analytical solutions a daunting task. Finally, increasing the complexity of the neuron model, for example, by considering biophysical models, is also extremely likely to prevent one from obtaining analytical results for the complete dynamics of the network, as these models have additional variables with complicated dynamics.

Future research will focus on the study of the traveling waves for more complex models of the neurons or in the presence of inhomogeneities, where the dynamics described here are subject to modulations induced by nonhomogenous kernels. For example, we considered weak, ϵ-order, periodic modulation of the connectivity. We have obtained preliminary results that indicate that while coupling between acceleration and speed remains similar, these additional ϵ-order terms modulate this interaction, leading to periodic modulation in the speed of the wavefront. More precisely, the wave speed oscillates above and below the fast stable solution from the homogenous case. Additional efforts will be aimed at obtaining analytical solutions for this type of equation. Finally, it would be interesting to see how other approaches, for example WKB methods that examine the evolution of a front based on a hyperbolic rescaling [47,48], relate to our approach and results. Additional question of interest are: how would these results translate for two-dimensional networks? What are the implications of considering populations of both excitatory and inhibitory neurons?

ACKNOWLEDGMENTS

This work was supported by a Georgia State Brain and Behavior Fellowship to J.Z., as well as by a Research Initiation Grant at Georgia State University, a Brain and Behavior Seed Grant at Georgia State University, and by a Early Career Award from the Mathematical Biosciences Institute at Ohio State University to R.O. We thank Michael Schwemmer for his useful suggestion of using our approach to examine the effect that a nonexcitable gap has on the further propagation of the waves.

[1] T. K. Sato, I. Nauhaus, and M. Carandini, Traveling waves in visual cortex, Neuron **75**, 218 (2012).

[2] T. Wanger, K. Takagaki, M. T. Lippert, J. Goldschmidt, and F. W. Ohl, Wave propagation of cortical population activity under urethane anesthesia is state dependent. BMC Neurosci. **14**, 78 (2013).

[3] J. B. Ackman and M. C. Crair, Role of emergent neural activity in visual map development. Curr. Opin. Neurobiol. **24**, 166 (2014).

[4] J. B. Ackman, T. J. Burbridge, and M. C. Crair, Retinal waves coordinate patterned activity throughout the developing visual system. Nature (London) **490**, 219 (2012).

[5] T. P. Zanos, P. J. Mineault, K. T. Nasiotis, D. Guitton, and C. C. Pack, A sensorimotor role for traveling waves in primate visual cortex, Neuron **85**, 615 (2015).

[6] I. Nauhaus, L. Busse, D. L. Ringach, and M. Carandini, Robustness of traveling waves in ongoing activity of visual cortex. J. Neurosci. **32**, 3088 (2012).

[7] A. Compte, M. V. Sanchez-Vives, D. A. McCormick, and X.-J. Wang, Cellular and network mechanisms of slow oscillatory activity (<1Hz) and wave propagations in a cortical network model. J. Neurophysiol. **89**, 2707 (2003).

[8] M. Murakami, H. Kashiwadani, Y. Kirino, and K. Mori, State-dependent sensory gating in olfactory cortex, Neuron **46**, 285 (2005).

[9] A. Reimer, P. Hubka, A. K. Engel, and A. Kral. Fast propagating waves within the rodent auditory cortex, Cerebral Cortex **21**, 166 (2011).

[10] M. Chrostowski, L. Yang, H. R. Wilson, I. C. Brue, and S. Becker, Can homeostatic plasticity in deafferented primary auditory cortex lead to traveling waves of excitation? J. Comput. Neurosci. **30**, 279 (2011).

[11] D. R. Belov, P. A. Stepanova, and S. F. Kolodyazhnyi, Traveling waves in the human eeg during voluntary hand movements, Neurosci. Behav. Physiol. **45**, 1043 (2015).

[12] D. Rubino, K. A. Robbins, and N. G. Hatsopoulos, Propagating waves mediate information transfer in the motor cortex, Nat. Neurosci. **9**, 1549 (2006).

[13] G. B. Ermentrout and D. Kleinfeld. Traveling Electrical Waves in Cortex, Neuron **29**, 33 (2001).

[14] K. Takahashi, M. Saleh, R. D. Penn, and N. G. Hatsopoulos, Propagating waves in human motor cortex, Front. Hum. Neurosci. **5**, 40 (2011).

[15] A. Bahramisharif, M. A. J. van Gerven, E. J. Aarnoutse, M. R. Mercier, T. H. Schwartz, J. J. Foxe, N. F. Ramsey, and O. Jensen, Propagating neocortical gamma bursts are coordinated by traveling alpha waves, J. Neurosci. **33**, 18849 (2013).

[16] M. Massimini, R. Huber, F. Ferrarelli, S. Hill, and G. Tononi, The sleep slow oscillation as a traveling wave, Front. Hum. Neurosci. **24**, 6862 (2004).

[17] V. L. Evgueniy and G. S. Athanassios, Hippocampal theta oscillations are traveling waves, Nature (London) **459**, 534 (2009).

[18] H. Zhang and J. Jacobs, Traveling theta waves in the human hippocampus, J. Neurosci. **35**, 12477 (2013).

[19] A. Keane and P. Gong, Propagating waves can explain irregular neural dynamics, J. Neurosci. **35**, 1591 (2015).

[20] F. H. Lopes da Silva, W. Blanes, S. N. Kalitzin, J. Parra, P. Suffczynski, and D. N. Velis, Dynamical diseases of brain systems: different routes to epileptic seizures, IEEE Trans. Biomed. Eng. **50**, 540 (2003).

[21] M. Ursino and G. E. La Cara, Traveling waves and EEG patterns during epileptic seizure: analysis with an integrate-and-fire neural network, J. Theor. Biol. **242**, 171 (2006).

[22] M. A. Dahlem and E. P. Chronicle, A computational perspective on migraine aura, Progr. Neurobiol. **74**, 351 (2004).

[23] J. R. Brasic, Hallucinations, Perceptual and motor skills **86**, 851 (1998).

[24] P. Tass, Oscillatory cortical activity during visual hallucinations, J. Biol. Phys. **23**, 21 (1997).

[25] K. P. Doyle, R. P. Simon, and M. P. Stenzel-Poore, Mechanisms of ischemic brain damage, Neuropharmacology **55**, 310 (2008).

[26] D. Cremers, Traveling waves of excitation in neural field models: equivalence of rate descriptions and integrate-and-fire dynamics, Neural Comput. **14**, 1651 (2002).

[27] S. Coombes, Waves, bumps, and patterns in neural field theories, Biol. Cybern. **93**, 91 (2005).

[28] H. G. E. Meijer and S. Coombes, Travelling waves in models of neural tissue: from localised structures to periodic waves, EPJ Nonlinear Biomed. Phys. **2**, 3 (2014).

[29] H. G. E. Meijer and S. Coombes, Travelling waves in a neural field model with refractoriness, J. Math. Biol. **68**, 1249 (2014).

[30] B. Ermentrout, The analysis of synaptically generated traveling waves, J. Comput. Neurosci. **5**, 191 (1998).

[31] P. C. Bressloff, Traveling waves pulses in a one-dimensional network of excitable integrate-and -fire neurons, J. Math. Biol. **40**, 169 (2000).

[32] R. Osan and G. B. Ermentrout, The evolution of synaptically generated waves in one- and two-dimensional domains, Physica D. **163**, 217 (2002).

[33] R. Osan, R. Curtu, J. Rubin, and G. B. Ermentrout, Multiple-spike waves in a one-dimensional integrate-and-fire neural network, J. Math. Biol. **48**, 243 (2004).

[34] R. Osan, R. Rubin, R. Curtu, and G. B. Ermentrout, Traveling waves in a one-dimensional integrate-and-fire neural network with finite support connectivity, Neurocomputing **52-54**, 869 (2003).

[35] R. Osan and G. B. Ermentrout, Speed-up methods for simulations of traveling waves in integrate-and-fire neural networks, Neurocomputing **52-54**, 863 (2003).

[36] R. Osan, J. Rubin, and B. Ermentrout, Regular traveling waves in a one dimensional network of theta neurons, SIAM J. Appl. Math. **62**, 1197 (2002).

[37] R. Osan and B. Ermentrout, Two dimensional synaptically generated traveling waves in a theta-neuron neural network, Neurocomputing **38-40**, 789 (2001).

[38] D. Golomb and Y. Amitai, Propagating neuronal discharges in neocortical slices: Computational and experimental study, J. Neurophysiol. **78**, 1199 (1997).

[39] L. R. Gonzalez-Ramirez, O. J. Ahmed, S. S. Cash, C. E. Wayne, and M. A. Kramer, A biologically constrained, mathematical model of cortical wave propagation preceding seizure termination, PLoS Comput. Biol. **11**, e1004065 (2015).

[40] P. C. Bressloff, *Waves in Neural Media: From Single Cells to Neural Fields* (Springer, New York, 2013).

[41] Z. P. Kilpatrick and B. Ermentrout, Response of traveling waves to transient inputs in neural fields, Phys. Rev. E **85**, 021910 (2012).

[42] P. C. Bressloff and M. A. Webber, Front propagation in stochastic neural fields, Soc. Ind. Appl. Math. **11**, 708 (2012).

[43] Z. P. Kilpatrick, Coupling layers regularizes wave propagation in stochastic neural fields, Phys. Rev. E **89**, 022706 (2014).

[44] D. J. Pinto and G. B. Ermentrout, Spatially structured activity in synaptically coupled neuronal networks, J. Soc. Ind. Appl. Math. **62**, 206 (2001).

[45] J. A. Villacorta-Atienza and V. A. Makarov, Wave-processing of long-scale information by neuronal chains, PLoS ONE **8**, e57440 (2013).

[46] J. E. Rubin, A Nonlocal Eigenvalue Problem for the Stability of Traveling Wave in Neuronal Medium, Discrete Contin. Dyn. Syst. **10**, 925, (2004).

[47] J. Xin, Front propagation in heterogeneous media, SIAM Rev. **42**, 161 (2000).

[48] V. Méndez, J. Fort, H. G. Rotstein, and S. Fedotov, Speed of reaction-diffusion fronts in spatially heterogeneous media, Phys. Rev. E **68**, 041105 (2003).